Vibrational Spectroscopy and Dynamics in the CH-Stretch Region of Fluorene by IVR-Assisted, Ionization-Gain Stimulated Raman Spectroscopy†

Taiho Kim and Peter M. Felker*

Department of Chemistry and Biochemistry, University of California, Los Angeles, California 90095-1569

Received: June 28, 2007; In Final Form: August 20, 2007

We report stimulated Raman spectra at 0.2 and 0.03 cm^{-1} resolution in the CH-stretching region of jet-cooled fluorene. The results were obtained by a version of ionization-gain stimulated Raman spectroscopy in which resonant two-photon ionization probing of the state-population changes arising from stimulated Raman transitions is assisted by the process of intramolecular vibrational redistribution (IVR) in the Raman-excited molecule. The fluorene spectra reveal extensive vibrational coupling interactions involving both the aliphatic and aromatic CH-stretching first excited states with nearby background states. Results pertaining to the symmetric aliphatic CH-stretching fundamental are consistent with a tier model of IVR and point to vibrational energy flow out of the CH stretch on a ∼1 ps time scale with subsequent redistribution on a ∼5 ps time scale.

I. Introduction

Intramolecular vibrational redistribution (IVR) has received considerable attention over the past several decades because of the centrality of the process in chemical and molecular relaxation dynamics. (For reviews, see refs 1−7.) Experimental methods to probe IVR are numerous and include powerful time-domain (e.g., refs 4 and 8−11) and frequency-domain (e.g., see refs 3, 5, and 7) schemes. However, notable gaps in the kinds of species and portions of the vibrational level structure that can be readily studied still exist. One such gap pertains to ground-state IVR in large molecules (e.g., polycyclic aromatic hydrocarbons). Time-domain methods suffer from the difficulty of exciting and probing the vibrational wavepackets associated with such species, especially in application to the sparse, collisionless samples that are most advantageous for the study of intramolecular dynamics. Frequency-domain methods also face obstacles in application to IVR studies of large molecules. Principal among these problems is the rotational congestion that enters into the spectra of such molecules and that masks the features associated with IVR. Although double-resonance schemes can be very effective in eliminating this rotational congestion[7] to produce spectra in which the structure due to (ro)vibrational couplings is plain (e.g., in application to species like benzene,[12] propargylamine,[13] and methylamine[14]), application of such methods to larger species is hindered by the large rotational partition functions that characterize the samples of such molecules, even those at the low temperatures achievable in seeded supersonic beams.

In this paper we demonstrate an approach to ground-state IVR studies of large species that is based on the measurement of stimulated Raman spectra. The principal advantage of this approach is the fact that the rotational band contours of totally symmetric Raman bands are generally dominated by single, narrow features associated with no change in rotational state during the vibrational transition (e.g., ^{Q}Q branches in symmetric tops[15]). The fractionation[3,5] of such a band by anharmonic coupling (i.e., IVR) produces multiple sharp features. Hence, even without rotational resolution the frequency-domain manifestations of IVR may be readily observable in Raman spectra. Given that spectral resolution on the order of 10^{-2} cm^{-1} is readily achievable in stimulated Raman schemes and that survey spectra over hundreds of cm^{-1} are straightforwardly measured, one has a means by which to investigate vibrational couplings and IVR timescales over a range of several orders of magnitude in large species.

The experimental method that we employ here is based on ionization-gain stimulated Raman spectroscopy (IGSRS),[16,17] a vibrational-vibronic double-resonance scheme in which the gain in population of excited vibrational states arising from stimulated-Raman transitions is monitored by resonantly enhanced two-photon ionization (R2PI). A key new aspect of the present work, distinguishing it from other IGSRS studies, is that it takes advantage of the IVR dynamics of the molecule to facilitate the R2PI probe process. Specifically, it relies on the vibronic spectral broadening that arises subsequent to dissipative IVR (e.g., see ref 2) to allow for fixed-frequency R2PI probing over wide regions of the stimulated-Raman spectrum. In conjunction with the prevalence of sharp rotational features in Raman spectra as described above, the (nominally) zero-background nature of this "IVR-assisted" IGSRS makes it very well-suited for measuring the congested vibrational spectra associated with IVR.

In this initial application of IVR-assisted IGSRS we study the fluorene molecule ($C_{13}H_{10}$) at ground-state vibrational energies between 2800 and 3300 cm^{-1}. This molecule is a good candidate for initial study in that IVR at vibrational energies up to about 2000 cm^{-1} in the S_1 manifold of fluorene has already been characterized with picosecond time-domain methods by Kauffman et al.[9] That group mapped out the transition from no IVR to restricted to dissipative IVR with increasing energy, measured IVR lifetimes in the ∼10 ps range for several states having ∼2000 cm^{-1} of vibrational energy and used a Fermi-golden-rule analysis to extract average vibrational coupling matrix elements. The results presented here extend these findings in several ways. First, the vibrational energies addressed herein are larger than those of ref 9. Second, the types of vibrational excitations studied here (aliphatic and aromatic CH-stretching

† Part of the "Giacinto Scoles Festschrift".

10.1021/jp075053i CCC: $37.00
Published on Web 10/09/2007

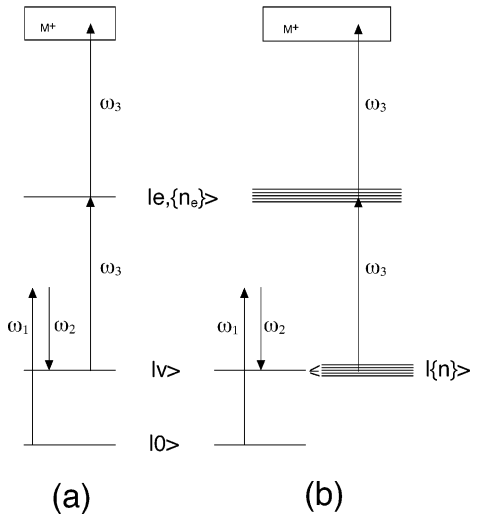

Figure 1. Level diagrams depicting the transitions involved in IGSRS. Excitation fields ω_1 and ω_2 drive a stimulated Raman transition from vibrational level $|0\rangle$ to $|v\rangle$ at the resonant frequency $\omega_1 - \omega_2$. (a) No IVR following excitation to $|v\rangle$. Raman-excited species are photoionized by ω_3 via R2PI originating in $|v\rangle$. (b) IVR following excitation to $|v\rangle$. Raman-excited species undergo IVR and are then photoionized by ω_3 via R2PI that originates in the states, $|\{n\}\rangle$, with which $|v\rangle$ is coupled and proceeds through the manifold of excited intermediate states $|e,\{n_e\}\rangle$.

fundamentals) were not studied in that earlier work. Third, the present work allows for the characterization of fluorene IVR processes into the subpicosecond regime. Finally, the ability here to measure spectra at 0.03 cm^{-1} resolution over tens of cm^{-1} makes plain the existence of hierarchies[18] in the pattern of vibrational couplings involved in fluorene IVR.

The paper is organized as follows. In the following section we describe more completely IVR-assisted IGSRS. In section III we outline the experimental apparatus and procedure employed to study jet-cooled fluorene. The final section is a presentation and discussion of the experimental results.

II. IVR-Assisted IGSRS

Figure 1a shows a level diagram depicting conventional IGSRS.[16,17] Laser fields ω_1 and ω_2 drive a stimulated Raman transition from $|0\rangle$ to $|v\rangle$. Laser field ω_3 is tuned to a vibronic transition originating in $|v\rangle$. By R2PI this latter field photoionizes those species excited to $|v\rangle$. Measuring the photoion signal vs $\omega_1 - \omega_2$ yields a stimulated Raman spectrum.

There are two difficulties[17] associated with conventional IGSRS. First, the vibronic spectra of different excited vibrational states $|v\rangle$, even ones close in energy, can be substantially different from one another. Thus, it is generally not possible to measure stimulated-Raman spectra over a range greater than several cm^{-1} without tuning ω_3. Second, if the Raman-excited vibrational states are subject to dynamical processes, the R2PI probe spectrum for a given $|v\rangle$ can evolve over the course of the experiment.

Figure 1b shows a level diagram depicting IVR-assisted IGSRS. In this scheme, one makes use of the fact that dissipative IVR originating in $|v\rangle$ tends to produce rapid (1 ns to <1 ps) evolution of the vibronic spectrum of the vibrationally excited molecule into one with broad features that do not substantially evolve further; see Figure 2. One also exploits the property that such a vibrationally "relaxed" vibronic spectrum is essentially independent of the identity of $|v\rangle$. Both of these properties of IVR-active molecules are well-known, for example, from measurements of single-vibronic-level fluorescence spectra of

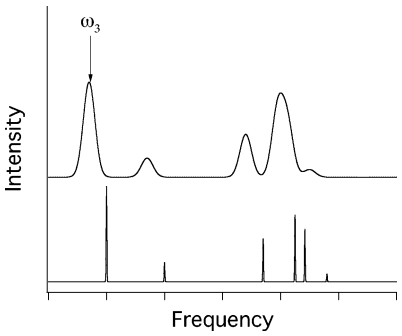

Figure 2. Schematic vibronic spectra corresponding to a ground-electronic-state molecule that is vibrationally unexcited (bottom) and excited to a vibrational level that undergoes dissipative IVR (top). The arrow indicates a frequency for ω_3 that is a suitable R2PI probe frequency for IVR-assisted IGSRS.

jet-cooled or gas-phase species.[2,8,19,20] They arise from the fact that due to IVR the "zero-order bright state" (ZOBS),[5] $|v\rangle$, rapidly evolves after excitation into a superposition of many other zero-order states having markedly different vibrational characters (the states $|\{n\}\rangle$ of Figure 1b). The highly diverse vibrational makeup of this superposition state is that which gives rise to the broad, vibrationally relaxed, vibronic spectrum orginating from it. The fact that in the dissipative IVR regime such diversity obtains regardless of the identity of $|v\rangle$ is that which renders the vibrationally relaxed vibronic spectra insensitive to $|v\rangle$'s nature. What these properties allow for in IGSRS is the ability to set ω_3 to a fixed frequency in the midst of a broad vibrationally relaxed vibronic band (e.g., the arrow in Figure 2) and by so doing measure Raman-induced increases in R2PI signals throughout the IVR-active vibrational level structure in the ground state. The excited vibrational-state dynamics eliminates the need to scan ω_3 simultaneously with $\omega_1 - \omega_2$, and the probe spectrum remains effectively constant in time after the initial, fast dissipative dynamics.

We note that the IVR-assisted IGSRS described above is very close to the stimulated-emission pumping−R2PI method employed by Bürgi et al.[21] to measure ground-state vibrational spectra and van der Waals binding energies in molecular complexes. In fact, their method is the resonance-Raman variant of the method described here. We note also the resemblance of the present scheme to the "nonresonant ionization detected infrared spectroscopy" developed by Fujii et al.[22] In the latter, the photoionization frequency is set to be slightly less than that required to photoionize from the zero-point level of the ground electronic state by two photons. Vibrational excitation by infrared absorption provides enough additional energy to allow two-photon ionization. Hence, ion signal vs IR frequency produces an IR-absorption action spectrum with fixed-frequency probing. The difference between their method and IVR-assisted IGSRS (apart from the vibrational excitation process) is that the former relies on probe processes that are not single-photon resonant as opposed to the R2PI probing employed here.

III. Experimental Section

The apparatus and methods employed for IGSRS experiments in this laboratory have been described in detail elsewhere.[23] Briefly, the ω_1 field was the frequency-doubled (532 nm) output of a 10 ns pulsed, injection-seeded Nd:YAG laser. The ω_2 field (628−645 nm) was the output of a dye laser pumped by the same Nd:YAG laser. The Raman resolution was determined by the bandwidth of the dye laser and was either 0.2 or 0.03 cm^{-1}

depending on whether the dye laser was tuned by a diffraction grating only or with a grating and an Etalon. The ω_3 field (298.5 nm) was the frequency-doubled output of a second dye laser pumped by a second Nd:YAG laser that was fired synchronously with the first. The ω_3 pulse was delayed such that it arrived at the sample approximately one pulse width after the arrival of the overlapped ω_1 and ω_2 pulses.

The sample consisted of a skimmed supersonic free-jet expansion of fluorene seeded in helium. Fluorene vapor at 100 °C was mixed with 300 psig helium (yielding about 1:100 fluorene:helium) in the pre-expansion region of a solenoid-driven pulsed valve (General Valve, Series 9) operating at 30 Hz. Expansion of the gaseous mixture into vacuum was through an orifice 0.08 cm in diameter. The expansion was skimmed several centimeters downstream whereupon it entered the differentially pumped ionization region of a Wiley−McClaren-type time-of-flight mass spectrometer. IGSRS spectra were collected by monitoring the fluorene parent-ion signal as a function of ω_2, with ω_1 and ω_3 held constant. In all experiments reported here ω_3, at 33 500 cm^{-1}, was about 275 cm^{-1} to the red of the $S_1 \leftarrow S_0$ 0_0^0band of fluorene.[24,25] At this ω_3 frequency the fluorene parent-ion signal was negligible whenever ω_1 and/or ω_2 were prevented from impinging on the sample.

IV. Results and Discussion

Prior to presenting experimental results it is useful to consider some background information pertaining to the CH-stretching vibrations of fluorene. There are two aliphatic and eight aromatic CH-stretching modes in fluorene. The former transform as A_1 and B_1 in the C_{2v} point group of the molecule.[26] One expects these fundamentals to be in the 2890−2940 cm^{-1} range with the A_1 band at lower frequency.[27] The aromatic CH stretches are composed of four A_1 and four B_2 modes. Ab initio calculations predict these fundamentals to lie within a ∼40 cm^{-1} window (about 3045−3085 cm^{-1})[27] and to be arranged in four doublets, with each doublet consisting of one B_2 and one A_1 fundamental separated from each other by ∼1 cm^{-1}.[28] This doublet pattern can be understood in terms of the separation of the two aromatic rings in fluorene and the expectation that such separation likely precludes strong couplings between CH stretching on the different rings.

In the absence of IVR the Raman spectra of the fluorene CH fundamentals should exhibit two qualitatively different types of bands at the resolution of the present work. The A_1 fundamentals should have band contours dominated by a single feature corresponding to the Boltzmann-weighted sum of rovibrational transitions of the type $|v;J_\tau\rangle \leftarrow |0;J_\tau\rangle$, where $|v;J_\tau\rangle$ represents an asymmetric-top rotational state $|J_\tau\rangle$ in the manifold of vibrational state $|v\rangle$.[15] The intensity of these bands should be significantly greater for parallel-polarized ω_1 and ω_2 fields ($I_{||}$) than for perpendicularly polarized ω_1 and ω_2 fields ($I_\perp$). In particular, $\rho \equiv I_\perp/I_{||} < 0.75$. In contrast the B_1 and B_2 fundamentals should both give rise to broad (several cm^{-1}) band contours without sharp features. And, their polarization ratios, ρ, should be equal to 0.75.[29] In the presence of IVR induced by anharmonic coupling[30] each of the fundamentals will fractionate into several bands, the number of which depends on the number of states effectively coupled to the excited CH stretch. The resulting bands should have contour shapes and polarization characteristics similar to the fundamental from which they arise.

Figures 3−7 show IVR-assisted IGSRS spectra of fluorene in three spectral regions above 2890 cm^{-1}. The spectra contain all the major Raman features observed from 2800 to 3300 cm^{-1} in this work. Those of Figures 3 and 4 correspond to the region of the two aliphatic CH-stretching fundamentals of the molecule. The spectra in Figures 5 and 6 correspond to the region of the aromatic CH-stretching fundamentals. And the Figure 7 spec-

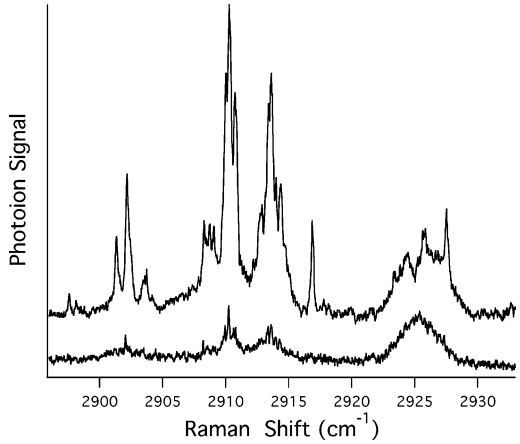

Figure 3. IVR-assisted IGSRS spectra of fluorene at 0.2 cm^{-1} resolution in the region of the aliphatic CH-stretching fundamentals. The top spectrum corresponds to parallel-polarized and the bottom to perpendicularly polarized ω_1 and ω_2 fields.

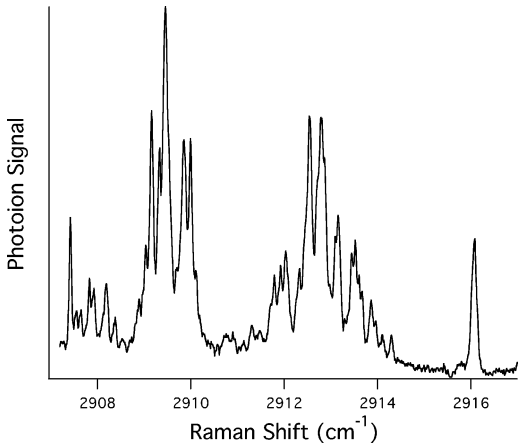

Figure 4. Portion at 0.03 cm^{-1} resolution of the IVR-assisted IGSRS spectrum of fluorene in the region of the aliphatic CH-stretching fundamentals. The ω_1 and ω_2 fields were parallel-polarized.

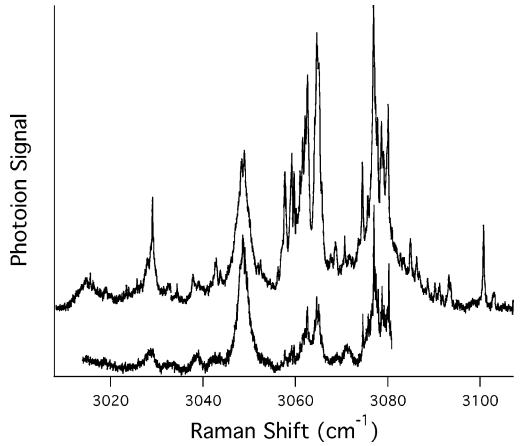

Figure 5. IVR-assisted IGSRS spectra of fluorene at 0.2 cm^{-1} resolution in the region of the aromatic CH-stretching fundamentals. The top spectrum corresponds to parallel-polarized and the bottom to perpendicularly polarized ω_1 and ω_2 fields. The latter is truncated on the blue end relative to the former.

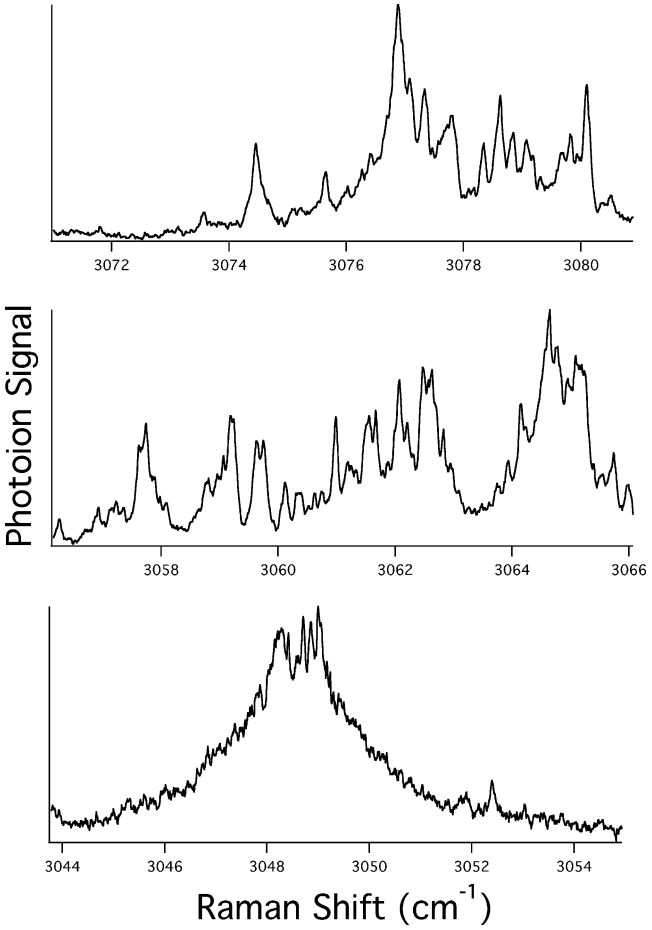

Figure 6. Three portions at 0.03 cm^{-1} resolution of the IVR-assisted IGSRS spectrum of fluorene in the region of the aromatic CH-stretching fundamentals. The ω_1 and ω_2 fields were parallel-polarized.

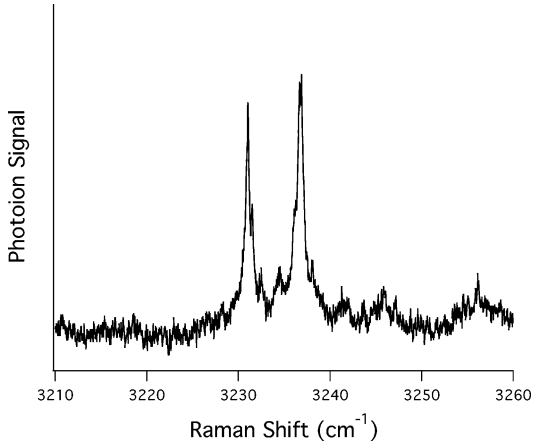

Figure 7. IVR-assisted IGSRS spectra of fluorene at 0.2 cm^{-1} resolution in the region of the first overtone of the ~1615 cm^{-1} A_1 vibrational mode. The spectrum corresponds to parallel-polarized ω_1 and ω_2 fields.

trum covers the region of the first overtone of the strong Raman-active CC-stretching mode whose fundamental is at about 1615 cm^{-1}.

There are several points to make about these results. First, there are many more Raman bands in the CH-stretching regions than there are CH-stretching fundamentals. This is plain from the lower-resolution spectra of Figures 3 and 5. It is even more apparent in higher-resolution results of Figures 4 and 6. This observation is no surprise given the extensive IVR to be expected[9] in fluorene at the relevant excitation energies. That vibrational coupling is the principal source of the observed congestion, as opposed to congestion due to combination bands and overtones with inherent transition strength, is strongly suggested by the dearth of similarly intense bands in neighboring spectral regions in which CH-stretching fundamentals are not present, that is, 2800−2890, 2930−3010, and 3110−3220 cm^{-1} (not shown).

Second, consider spectral assignments in the aliphatic CH-stretch region. The many sharp bands in Figures 3 and 4 with small ρ values can be confidently attributed to transitions ending in totally symmetric vibrational states (A_1 in the C_{2v} point group of the molecule[26]). We assign these bands, which have a "center of gravity" at about 2910 cm^{-1}, as being due to the IVR-split, aliphatic CH-stretching fundamental of A_1 symmetry. In contrast, the unpolarized, broad feature at 2925 cm^{-1} (see Figure 3) arises from nontotally symmetric vibrational excitation(s). We assign it as being associated with the asymmetric aliphatic CH-stretching fundamental of B_1 symmetry. In fact, it is almost certainly a superposition of several B_1 bands deriving their intensity from vibrational coupling with the excited B_1 CH-stretching state. However, the inherent breadth of the rotational contours of B_1 bands (in contrast to the sharp A_1 band contours) precludes any definitive assessment of the feature's composition.

Third, the assignment of features in the region of the aromatic CH-stretching fundamentals (Figures 5 and 6) is complicated by the number of such fundamentals and by the congestion arising from vibrational couplings. Nevertheless, the polarization-specific spectra of Figure 5 give one a start in making such assignments. In particular, the strongly polarized features in the clumps centered near 3062 and 3077 cm^{-1} are certainly due to A_1 bands. The large intensities of these features strongly suggest that they are due to two (or more) IVR-fractionated A_1 CH-stretching fundamentals. One sees that there are also other strongly polarized sharp features in other parts of the aromatic CH-stretching region. The provenance of these A_1 bands cannot be sorted out in detail here, though most, if not all, are also very likely the result of fractionated aromatic CH fundamentals. As to bands deriving from the B_2 fundamentals one notes, in particular, the broad, unpolarized feature centered at 3048 cm^{-1}. It is most likely the result of overlapping B_2 bands arising from the IVR-induced fractionation of a B_2 CH-stretching fundamental. Other B_2 features are almost certainly present in the spectra of Figure 5. Unfortunately, there is no way here to distinguish between B_2 bands and the unpolarized portions of A_1 bands when the two band types overlap spectrally.

Fourth, the last major bands observed in this work are those evident in Figure 7. These are about one-third as intense as the stongest bands in the aliphatic and aromatic CH-stretching regions. There is little doubt that these bands are associated with the first overtone of the A_1 fundamental near 1615 cm^{-1}. That fundamental has been observed with very strong intensity in the Raman spectra of fluorene in CCl_4 solution (at 1615 cm^{-1}) and in the pure crystal (at 1612 cm^{-1}).[26]

Finally, consider in more detail the information that the present results contain regarding vibrational couplings and IVR at energies above 2900 cm^{-1} in fluorene. We focus specifically on the A_1 bands in the aliphatic CH-stretching region (see Figures 3 and 4), because they can be reasonably attributed to the fractionation of a *single* ZOBS, namely, the first excited state of the aliphatic symmetric CH stretch. One notes, in particular, the hierarchical nature of the A_1 band structure in this region. It consists of several "clumps" spread out over ~15 cm^{-1}, each of which in turn consists of finer structure spaced by tenths of cm^{-1} over ranges of 1−2 cm^{-1}. Such results are

consistent with a tier model of IVR (e.g., refs 3, 5, 6, and 11b), in which vibrational energy flow out of the ZOBS proceeds first through nearby zero-order states (Tier 1) strongly coupled to it through low-order anharmonicities. (The spectral manifestation of this is the gross clump structure in Figure 3.) This is followed by energy flow from the Tier-1 states into a second set of nearby zero-order states (Tier 2) similarly strongly coupled to them, etc. (This is manifested spectrally by the structure within the clumps; see Figure 4.) The experimental results imply a time scale on the order of $\Gamma^{-1} \simeq 1/2\pi c \times 5\ \mathrm{cm}^{-1} \simeq 1$ ps for the ZOBS-to-Tier 1 redistribution and a Tier 1-to-Tier 2 redistribution time about 5 times slower.[31] The former time scale can be compared with the 10 ps decay times measured by Kauffman et al.[9] in their time-domain study of ZOBS survival probabilities at vibrational energies near 2000 cm^{-1} in S_1 fluorene. The order-of-magnitude decay-rate increase for the excited CH stretch is not unreasonable given the considerable increase in the vibrational density of states in going from 2000 to 2900 cm^{-1}.

It is of interest to make a connection between the apparent hierarchical nature of the aliphatic CH-stretch IVR and the fluorene vibrational level structure. By using direct state counting along with fluorene vibrational frequencies from ref 26, one can compute the number of A_1 vibrational states in the vicinity of 2910 cm^{-1}. Although the total number of such states is about 5500 states per cm^{-1}, the number of states differing by only three vibrational quanta from the first excited CH-stretching state is very much smaller. One finds five such states available for low-order anharmonic coupling with the ZOBS in the interval from 2903 to 2931 cm^{-1}. The inclusion of states differing by four quanta from the ZOBS adds an additional three states per cm^{-1}. Given that only a fraction of these $\Delta v = 4$ states might be expected to couple strongly with the CH stretch, one sees that the number of low-order coupling resonances implied by the state-counting calculation is consistent with the gross clump structure (Tier-1 structure) observed in the spectra. As for the Tier-2 structure, the number of bands observed (see Figure 4) is obviously much less than that implied by the total density of A_1 states, a fact consistent with the considerable selectivity to be expected in Tier-1/Tier-2 coupling. Beyond Tier 2 our experimental resolution is insufficient to reveal any further splittings. It is important to note, though, that such fine structure very likely is present, given that numerous studies have found that the density of vibrational bands due to IVR fractionation is of the order of the density of vibrational states in the molecule (see, e.g., refs 3 and 5).

One last point about IVR in the CH-stretching region of fluorene is noteworthy. There is a substantial difference in its characteristics when compared with the IVR involving CH-stretching fundamentals in substituted acetylenes. A considerable body of results exists pertaining to the latter.[3,11] Indeed, such results represent perhaps the most extensive data set relating to IVR following CH-stretch excitation. They reveal IVR lifetimes of tens to hundreds of picoseconds or, equivalently, fractionation bandwidths of tenths to hundredths of cm^{-1}. These numbers are 1−2 orders of magnitude different than the analogous fluorene numbers. In contrast, results pertaining to the first overtones of CH stretches in single-ring aromatics[32] are more similar to the fluorene results reported here in that they indicate ZOBS decay on a subpicosecond time scale followed by slower redistribution on a 10−20 ps time scale. The wide range of IVR parameters associated with different kinds of species adds to the evidence for the intuitive expectation that there are structure-specific influences on vibrational couplings and dynamics. The unraveling of those influences can only benefit from the characterization of IVR for a wide range of species and vibrational excitations. The experimental approach presented in this paper can play a valuable role in this endeavor.

Acknowledgment. We are grateful to P. H.-Y. Cheong for performing *ab initio* calculations relating to the harmonic vibrational frequencies of fluorene in its ground state.

References and Notes

(1) McDonald, J. D. *Annu. Rev. Phys. Chem.* **1979**, *30*, 29.
(2) Smalley, R. E. *Annu. Rev. Phys. Chem.* **1983**, *34*, 129.
(3) Lehmann, K. K.; Scoles, G.; Pate, B. H. *Annu. Rev. Phys. Chem.* **1994**, *45*, 241.
(4) Felker, P. M.; Zewail, A. H. In *Jet Spectroscopy and Molecular Dynamics*; Hollas, J. M., Phillips, D., Eds.; Blackie A&P: London, 1995.
(5) Nesbitt, D. J.; Field, R. W. *J. Phys. Chem.* **1996**, *100*, 12735.
(6) Gruebele, M.; Bigwood, R. *Int. Rev. Phys. Chem.* **1998**, *17*, 91.
(7) Keske, J. C.; Pate, B. H. *Annu. Rev. Phys. Chem.* **2000**, *51*, 323.
(8) Felker, P. M.; Zewail, A. H. *J. Chem. Phys.* **1985**, *82*, 2961. Felker, P. M.; Zewail, A. H. *J. Chem. Phys.* **1985**, *82*, 2975. Felker, P. M.; Zewail, A. H. *J. Chem. Phys.* **1985**, *82*, 3003.
(9) Kauffman, J. F.; Côté, M. J.; Smith, P. G.; McDonald, J. D. *J. Chem. Phys.* **1989**, *90*, 2874.
(10) Smith, P. G.; McDonald, J. D. *J. Chem. Phys.* **1990**, *92*, 1004.
(11) (a) Yoo, H. S.; DeWitt, M. J.; Pate, B. H. *J. Phys. Chem. A* **2004**, *108*, 1348. (b) Yoo, H. S.; DeWitt, M. J.; Pate, B. H. *J. Phys. Chem. A* **2004**, *108*, 1365. (c) Yoo, H. S.; McWhorter, D. A.; Pate, B. H. *J. Phys. Chem. A* **2004**, *108*, 1380.
(12) Callegari, A.; Srivastava, H. K.; Lehmann, K. K.; Scoles, G.; Davis, M. J. *J. Chem. Phys.* **1997**, *106*, 432.
(13) Andrews, A. M.; Fraser, G. T.; Pate, B. H. *J. Chem. Phys.* **1998**, *109*, 4290.
(14) Merker, U.; Srivastava, H. K.; Callegari, A.; Lehmann, K. K.; Scoles, G. *Phys. Chem. Chem. Phys.* **1999**, *1*, 2427.
(15) For example, see: Herzberg, G. *Molecular Spectra and Molecular Structure, Vol. II. Infrared and Raman Spectra of Polyatomic Molecules*; Van Nostrand Reinhold: New York, 1945.
(16) Esherick, P.; Owyoung, A. *Chem. Phys. Lett.* **1983**, *103*, 235. Esherick, P.; Owyoung, A.; Pliva, J. *J. Chem. Phys.* **1985**, *83*, 3311.
(17) Hartland, G. V.; Henson, B. F.; Venturo, V. A.; Hertz, R. A.; Felker, P. M. *J. Opt. Soc. Am. B* **1990**, *7*, 1950.
(18) Davis, M. J. *J. Chem. Phys.* **1993**, *98*, 2614.
(19) Parmenter, C. S. *Faraday Discuss. Chem. Soc.* **1983**, *75*, 7.
(20) Felker, P. M.; Zewail, A. H. *Chem. Phys. Lett.* **1984**, *108*, 303.
(21) For example, T. Bürgi, T.; Droz, T.; Leutwyler, S. *J. Chem. Phys.* **1995**, *103*, 7228.
(22) Omi, T.; Shitomi, H.; Sekiya, N.; Takazawa, K.; Fujii, M. *Chem. Phys. Lett.* **1996**, *252*, 287. Ishiuchi, S.; Shitomi, H.; Takazawa, K.; Fujii, M. *Chem. Phys. Lett.* **1998**, *283*, 243.
(23) For example, Kim, W.; Schaeffer, M. W.; Lee, S.; Chung, J. S; Felker, P. M. *J. Chem. Phys.* **1999**, *110*, 11264.
(24) Amirav, A.; Even, U.; Jortner, J. *Chem. Phys.* **1982**, *67*, 1.
(25) Meerts, W. L.; Majewski, W. A.; van Herpen, W. M. *Can. J. Phys.* **1984**, *62*, 1293.
(26) Bree, A.; Zwarich, R. *J. Chem. Phys.* **1969**, *51*, 912. The axis convention employed in this reference and herein has the *z* axis as the short, in-plane axis, and the *x* axis as the axis perpendicular to the molecular plane.
(27) See: Guchhait, N.; Ebata, T.; Mikami, N. *J. Phys. Chem. A* **2000**, *104*, 11891. Application of a CH scaling factor of 0.91 (e.g., see the web site http://srdata.nist.gov/cccbdb/vsf.asp) to the calculated fluorene frequencies reported therein yields the frequency ranges quoted in the text.
(28) Cheong, P. H.-Y. Private communication.
(29) This discussion neglects the possibility that the intense stimulated-Raman fields might transform the free rotational states of the molecule into optical-field-induced pendular states so that the observed band contours are pendular contours rather than rotational contours. Nevertheless, the qualitative characteristics of totally symmetric vs nontotally symmetric Raman bands (i.e., sharp vs broad, polarized vs unpolarized) apply also to pendular contours. See: Kim, W.; Felker, P. M. *J. Chem. Phys.* **1996**, *104*, 1147.
(30) We neglect rovibrational couplings here (e.g., Coriolis coupling) because such couplings are so small as to give rise to spectral structure that cannot be resolved in the present experiments. For example, see ref 6, eq 1.2, and the related text.
(31) 5 cm^{-1} is roughly the effective width of the A_1 structure associated with the aliphatic CH-stretching fundamental in Figure 3. The widths of the clumps are about 1 cm^{-1}.
(32) Callegari, A.; Merker, U.; Engels, P.; Srivastava, H. K.; Lehmann, K. K.; Scoles, G. *J. Chem. Phys.* **2000**, *113*, 10583; **2001**, *114*, 3344.